DESIGN STUDY OF THE UELV-10/5-15S ACCELERATING STRUCTURE

I.O. Chetverikov, M.A. Kalinichenko, A.V. Ryabtsov, Yu.V. Zuev
NIIEFA D.V. Efremov Scientific Research Institute of Electrophysical Apparatus
St-Petersburg, Metallostroy, av. Sovetsky 1, Russia
e-mail: NPK LUTS @ NIIEFA. SP.SU

The UELV-10/5-15S electron linear accelerator is intended for use in the sterilization applications. Electron energy can be continuously variable from 5 to 10 MeV by changing the accelerated beam current. The 2 m long accelerating structure includes a standing wave buncher, a travelling wave accelerating part and an on-axis resonant RF load. Beam dynamics calculations have been made taking into account space charge forces. Optimization of the buncher parameters permitted to achieve capture efficiencies up to 75% with no external focussing. It is expected that beam powers from 13 kW to 15 kW will be obtained in the 5 to 10 MeV energy range.
PACS number: 29.17.+w

1 INTRODUCTION

The UELV-10/5-15S electron linear accelerator with a combined accelerating structure [1] is designed for different irradiation uses, in particular for sterilization applications. The electron energy may be continuously varied from 5 to 10 MeV by changing the accelerated beam current from 0.58 to 0.33 A. The average beam power is 13-15 kW. The beam focusing in all modes is accomplished by the accelerating RF-field.

The klystron KIU-147A with parameters 6 MW, 25 kW, 2856 MHz is used as an accelerator RF-source. The peak and average RF-powers supplied to the accelerating structure are 4.7 MW and 22.5 kW, respectively. The repetition rate is 300 Hz, the pulse duration is 16 µs. The electron source is a 50 kV diode gun with a maximum beam peak current of 0.9 A. High voltage is applied to the gun from the klystron modulator. Magnetic coil is placed in the 200 mm gap between the gun and the input collimator of the structure. Choice of the coil current and coil position determines the necessary current of the injected beam and optimum matching of the input transverse phase ellipse with structure acceptance.

The 2054.8 mm accelerating structure consists of 82 cells. The structure can be divided into three sections: a buncher, an accelerating part and a resonant RF-load.

2 BUNCHER

The buncher consists of 11 cells, including the #11 coupler cell. The buncher operates in the $\pi/2$ standing wave mode. The cell dimensions and field amplitudes have been found as a result of transverse and longitudinal particle dynamics optimization. The purpose of this optimization was to achieve a narrow electron energy spectrum (3-4%), with the bunch phase width of about 20°. The narrow energy spectrum facilitates beam control problems and allows the beam to be used more effectively in the technological processes. Furthermore, the moderate bunch phase width supports repulsive space charge forces at the acceptable level. The initial optimization of the transverse beam dynamics (with no space charge forces) has been made to arrange the overfocusing in the region where the electron energy is from 2 to 3 MeV. Coulomb forces in the subrelativistic intense beam counteract to the overfocusing and are capable to increase the current fraction passing through the structure provided that small correction of the buncher parameters were made.

The specific feature of a buncher in the combined structure is the weak dependence of the field amplitudes and phases on the beam current. High- quality accelerated beams in the energy range from 5 to 10 MeV should be obtained due to this feature.

3 ACCELERATING PART

The accelerating part operates in the travelling wave $\pi/2$ mode and comprises the cells from the 12th to the 70th inclusive. The part geometry is of quasi- constant gradient design. Compared to more traditional cylindrical geometry U-shape cells have higher Q-factors and shunt-impedances. The accelerating part contains four uniform $\pi/2$ mode segments of increasing impedance interconnected by transition groups of 3 cells each. Table 1 lists neighbor coupling coefficients $k_{n,n+1}$, quality factors Q_n and shunt-impedances $r_{s,n}$ for cells of each segment.

Table 1

Cell numbers	$k_{n,n+1}$	Q_n	$r_{s,n}$,MΩ, m
12÷28	0.035	11260	1.030
32÷46	0.020	11224	1.084
50÷56	0.012	11208	1.118
60÷66	0.0063	11198	1.138

4 RESONANT LOAD

A build-in on-axis resonance load consisting of 12 cylindrical $\pi/2$-mode cells coated by Al-Si-Fer is used in the UELV-10/5-15S electron linear accelerator. A uniform power dissipation per cell has been assumed at zero beam current. The endurance of coating is determined by the surface density of RF-losses q. To reduce q it is necessary to increase coating area. It results, in turn, in the lowering of field amplitude in the load. The latter has been obtained by increasing the coupling coefficient up to k = 0.027. The Q-values of load cells have been calculated by the method described in [2] and are listed in Table 2.

Table 2

ВОПРОСЫ АТОМНОЙ НАУКИ И ТЕХНИКИ. 2001. №5.
Серия: Ядерно-физические исследования (39), с. 106-108.

106

cell №	71	72	73	74	75	76
Q	889	747	735	605	580	463
cell №	77	78	79	80	81	82
Q	426	322	273	181	121	45

Comparison shows that the q value in the UELV-10/5-15S accelerator is twice as less than that in the operating UELV-8-2D-30 linear accelerator. However, average RF-losses in the UELV-10/5-15S (10.53 kW) are five times higher than that in the UELV-8-2D-30 (2.14 kW). Excessive heating should be taken away by water flow cooling the accelerating part of the structure. In this case the temperature drop between the load walls and water increases by a factor of 2.5, but the frequency detuning caused by this drop will not considerably affect the load operation because of low Qs of the load cells.

These measures have to provide the reliable load operation especially as zero beam-loading mode is not nominal for the structure. The data of table 3 compare RF-power losses in the accelerating part and resonant load for three operational modes.

Table 3

Pulse beam current, A	0	0.33	0.58
Average RF-losses power on the accelerating part, kW	11.97	5.50	3.4
Average RF-losses power on the load, kW	10.53	0.43	3.4

Note, that Joule losses in the load are negligible for 10 MeV mode, and are three times less for 5 MeV mode than that for the zero beam-loading mode.

It is essential that RF-field in the build-in load affects the electron energy. In particular, an addition energy gain in 10 MeV mode is 0.2 MeV while deceleration in the load in 5 MeV mode gives an electron energy loss of 1.1 MeV. So, the range of beam current variation at injection becomes narrower to provide the accelerated beams of high quality in all modes.

5 STRUCTURE CHARACTERISTICS

The cells connecting uniform segments of accelerating waveguide define the frequency band properties of the combined accelerating structure. Calculations show, that the VSWR values at zero beam current do not exceed $\beta_0 \leq 1.2$ over the frequency band of 2856±0.45 MHz (Fig. 1). That is quite sufficient to ensure the normal operation of accelerator because of high- frequency stability of the RF-field ($\Delta f/f_0 \approx 1 \cdot 10^{-6}$) and when using the automatic frequency control system.

The final optimization of beam dynamics of the accelerator has been made taking into account the Coulomb forces. The beam continuously injected has been simulated by 3000 large charged particles. The optimization goal was to maximize the number of particles passing through the structure. To achieve this goal it was necessary to correct the buncher parameters and to inject into the structure a converging beam of a rather large diameter. The latter permits to relax the transverse Coulomb repulsion forces in the beginning of the

buncher, where the electron bunches are formed. The maximum accelerated beam current has been obtained at the injected beam diameter of 7 mm and initial convergence angles of (-25) mrad and (-10) mrad in the 5 and 10 MeV operational modes, respectively.
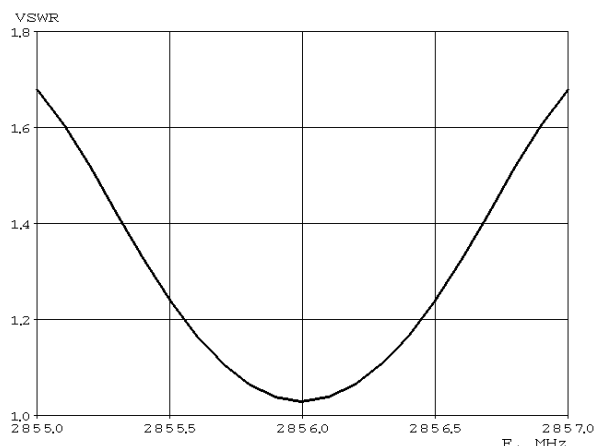

Fig. 1. VSWR-frequency dependence of UELV-10/5-15S.

Generally, space charge effects are considered as parasitic ones, which deteriorate beam parameters. However, in this case the space charge was included from the very beginning of optimization, and it results in the improvement of beam current passing through the structure while increasing injected current from 0.5 to 0.9 A (75.4% and 78.7%, respectively). Particularly, 90% of accelerated electrons were found inside the spot of 9.6 mm diameter (5 MeV mode) and 11.5 mm diameter (10 MeV mode). The beam at the accelerator output is divergent in all modes.

The nonlinear distortions of phase volume of accelerated beam are minimum because of high operational buncher quality (Figs. 2, 3). The beam diameter at the output foil window is estimated of 15-20 mm taking into account the beam divergence and relevant drift space. It diminishes the foil heating and, therefore, extends its lifetime and improves the uniformity of object irradiation.
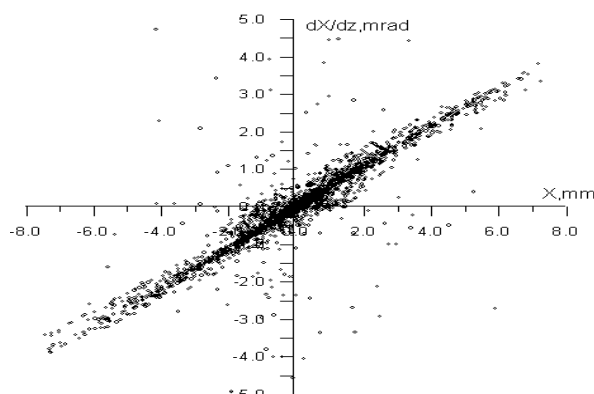

Fig. 2. The beam phase portrait at the accelerating structure output (10 MeV mode).
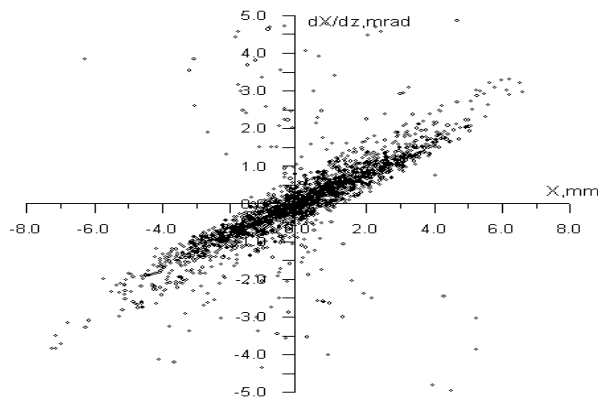
Fig. 3. The beam phase portrait at the accelerating structure output (5 MeV mode).

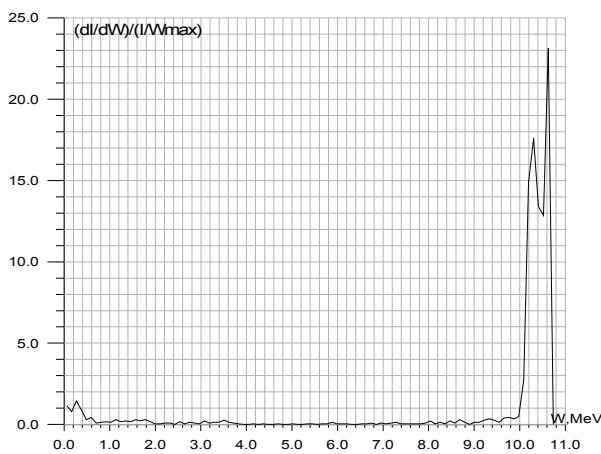The beam energy spectra at the nominal modes are shown in Figs. 4, 5.
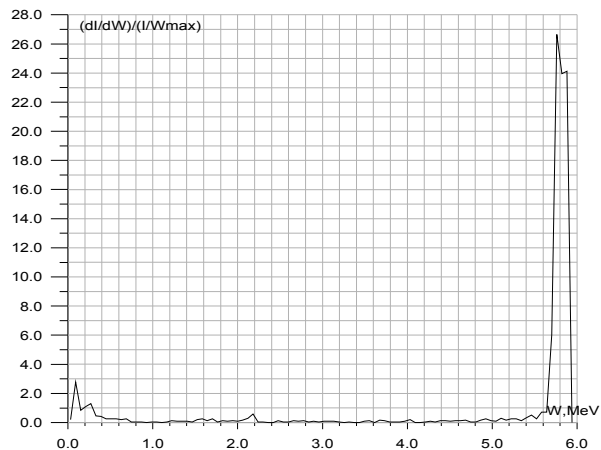

Fig. 4. The beam energy spectrum (10 MeV).

Fig. 5. The beam energy spectrum (5 MeV).

The beam loading and beam power characteristics of

The measured bandwidth at VSWR<2 is about octave. HOM damping efficiency was measured by S-parameters method using P2-83 network analyser and low-coupling antennas. Figure 3 presents the measurement results for S21 parameter within a frequency range.

HOM quality factors within 0.9–2.2 GHz frequency range (i.e. within the range where HOMs with large R/Q value are located) do not exceed 100 for the most HOMs. The fundamental mode (E_{110}) quality factor de-

the UELV-10/5-15S accelerator are shown in Fig. 6. The curves are calculated for the pulse duration of 14 μs.
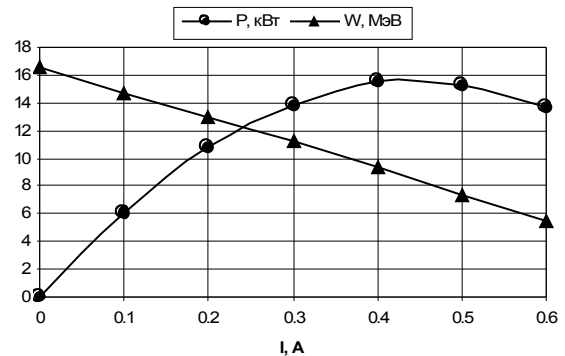

Fig. 6. The load and power characteristics of the UELV-10/5-15S accelerator.

The maximum of beam average power of 15.5 kW was found at 8.5 MeV. Suggesting the average RF-power fed into the structure was 22.6 kW the maximum electron efficiency of π/2-structure has been found as 68%. The average beam powers amount to 14.3 kW and 13.0 kW when the electron energies are 10.3 MeV and 5.2 MeV, respectively.

6 CONCLUSION

The optimization of the accelerating structure permits to achieve the required beam characteristics without external focusing. Calculated capture efficiencies are about 75% for both nominal modes. The total length of the structure is 2.05 m.

The accelerating structure of the UELV-10/5-15S linear electron accelerator is now in fabrication.

REFERENCES

1. Yu.P.Vakhrushin, A.V.Ryabtsov, V.L.Smirnov, V.V.Terent'ev. Combined Accelerating Structure With Optimized Multicavity Buncher // *Proc. XIII All-Russia Workshop on Charged Particle Accelerators*, Dubna, 1992, v 1, p. 249 (in Russian).
2. A.V.Ryabtsov. Calculating of Resonant Loads in The Traveling Running Wave Linear Electron Accelerator // *Proc. XVII All-Russia Workshop on Charged Particle Accelerators*, Protvino, 2000 (in Russian).

creasing when connecting the loads to the wave-to-coax transition is about 7.5%.

4 CAVITY TESTING

After assembling, the cavity was heated at workbench during 24 hours at a temperature of 150ºC, and then inserted into the damping ring and connected to the systems of RF power supply, water cooling, and control. Vacuum 160 l/s ion pump provided 10^{-9} Torr vacuum

ВОПРОСЫ АТОМНОЙ НАУКИ И ТЕХНИКИ. 2001. №5.
Серия: Ядерно-физические исследования (39), с. 108-108.

108

without RF. Conditioning was started in pulsed mode, which prevented discharge path memorizing, limited discharge energy, and allowed us to provide the required pressure level by varying the relative pulse duration. After 2 hour conditioning the nominal voltage of 300 kV in continuous mode was obtained in the cavity at pressure of 10^{-8} Torr. The reflection coefficient in the cavity power supply feeder line corresponded to the one measured at low power level. The maximal heating was observed at a place of waveguide connection. Frequency detuning at 20 kW dissipating power level was – 150 kHz. The general view of the cavity is shown in Fig. 4.
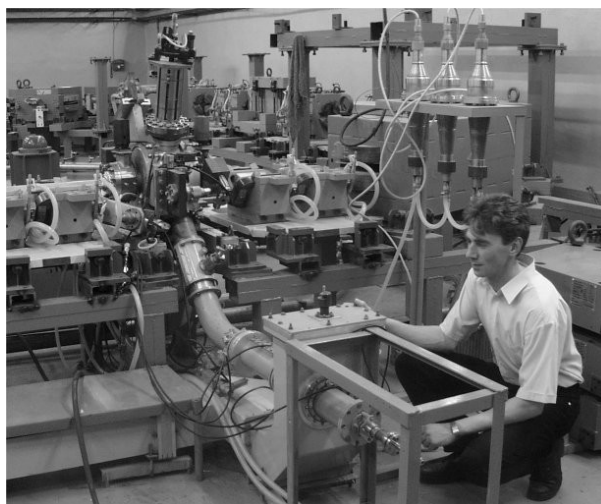

Fig. 1. General view of the cavity.

REFERENCES

1. N.S.Dikansky et al. // *Proc. of EPAC'94*, Jule 1, 1994, London, p. 482–484.
2. V.V.Parkhomchuk et al. Status of the injector complex for c/τ-factory at Novosibirsk // *Proc. APAC'98*, March 23–27, Tskuba, Japan, 1998.
3. A.Alinovsky et al. RF system for VEPP-5 damping ring // *Proc. of PAC'98*, 22–28 June, 1998, Stockholm.
4. D.Myakishev and V.Yakovlev // *Proc. PAC'91*, May 6–9, San-Francisco, p. 3002.